

Reaction and barrier formation at metal-GaP(110) interfaces

K. E. Miyano, R. Cao, T. Kendelewicz, A. K. Wahi, I. Lindau, and W. E. Spicer

Stanford Electronics Laboratories, Stanford University, Stanford, California 94305

(Received 10 April 1989)

The interfacial chemistry of Cu, Ag, Au, Ni, Pd, Al, Ga, In, Sn, and Bi deposited on cleaved GaP(110) surfaces has been studied using soft-x-ray photoemission spectroscopy. Of the noble metals, Cu and Au tend to disassociate the GaP, whereas the Ag shows little sign of reactivity with the substrate. The transition metals Ni and Pd react strongly with the GaP to form phosphides in which Ga is segregated. Of the column-III overlayers, Ga and In display strong clustering and little reactivity with the substrate, but the interface with Al shows a cation replacement reaction similar to that seen at Al/GaAs(110). Sn and Bi exhibit Stranski-Krastanov growth, with the establishment of metallic islands on a laminar first monolayer. Despite the differences in reactivity, the barrier heights for all the metals but In are observed to stabilize in the range of 1.14 to 1.46 eV. Hence the *n*-type GaP barrier height shows a much weaker dependence on the overlayer work function than reported previously. As with GaAs(110) this Fermi-level stabilization position is in the range of both the defect levels as created by irradiation, and the theoretical charge neutrality level toward which metal-induced gap states should move the surface Fermi level. The influence of overlayer reactivity, morphology, and metallicity on the barrier development is discussed in relation to these two potential sources of interface states.

I. INTRODUCTION

The barrier heights at interfaces between metals and GaAs(110) and InP(110) interfaces have displayed only a weak dependence on the electronegativity or work function of a wide range of metals. Various explanations have been proposed for this weak dependence, two of which are a defect mechanism^{1,2} and metal-induced gap states (MIGS).³⁻⁶ Recently, however, it has been suggested that barrier heights in systems involving other semiconductors may exhibit a much stronger dependence on the overlayer material.⁷⁻⁹ In particular, a previous photoemission experiment by Chiaradia *et al.*⁸ and Brillson *et al.*⁹ has indicated that Schottky-barrier heights on GaP(110) exhibit a near-perfect correspondence to the overlayer metal work function. In this present work the detailed chemistry of GaP is examined for ten overlayer materials and compared to that of GaAs and InP. Understanding of the interfacial chemistry is critical to these photoemission-based Schottky-barrier investigations for several reasons. First of all identification of chemically shifted components in the core-level spectra is necessary to extract the band bending from these spectra. Secondly, the chemical reactions at metal-III-V interfaces are expected to play a role in determining the Fermi-level movement and stabilization. For example, with the Ag-*n*-type InP system the reactivity may be significantly reduced by lowering the substrate temperature, and this reduced reactivity results in the final barrier height changing from the defect-induced level observed at room temperature to a higher position associated with MIGS.¹⁰ Another crucial aspect of the chemistry is the nature of the adatom surface bonding and its determination of the overlayer morphology. In the case of highly reactive overlayers the adatoms tend to have a low surface mobili-

ty, whereas certain nonreactive adatoms such as In cluster readily on the surface. Clustering affects the coverage at which the overlayer acquires characteristics of the bulk metal, and several authors have considered this achievement of "metallicity" to coincide with the onset of MIGS.^{11,12}

The chemistry of the interfaces examined in this study will be reviewed below with analogies and comparisons made to past Schottky-barrier work on the heavily studied substrates of GaAs(110) and InP(110). These systems are particularly appropriate for comparison because chemical shifts appearing in the Ga 3*d*-spectra, for say, a Ni overlayer, are expected to be similar for GaP and GaAs. Similarly the earlier InP work provides a reference for chemical shifts observed in the GaP P 2*p* spectra.

Once the interfacial chemistry at these metal-GaP interfaces was understood, the "bulk" components of the Ga 3*d* and P 2*p* core-level spectra were isolated, and their shifts after each overlayer deposition were measured: thus the Schottky-barrier formation was determined as a function of metal coverage. We found for the ten overlayers in this study a much weaker dependence of the final barrier height on overlayer material than reported in the previous photoemission experiments,^{8,9} with the exception of In, the other overlayers provide a barrier-height variation of only 0.3 eV despite a range of overlayer work functions covering 0.95 eV (from 4.2 eV for Ga to 5.15 eV for Ni). Barrier-height discrepancies between the previous work and the present are attributed to differing interpretations of chemical shifts in the substrate core-level spectra: our interpretations of these shifts are justified in detail below.

Hence we have observed Fermi-level "pinning" at GaP(110) interfaces, and this pinning is discussed in terms of the interplay of defects induced by the metal

deposition and MIGS, just as for Schottky barriers on GaAs(110) and InP(110). Our detailed studies of the interfacial chemistry provides information in regard to overlayer reactivity, morphology, and metallicity: such information can help in various instances to distinguish between the two mechanisms.

II. EXPERIMENT

These photoemission experiments were performed at the Stanford Synchrotron Radiation Laboratory using soft x rays from a grasshopper monochromator. A standard UHV chamber equipped with a double-pass cylindrical mirror analyzer was utilized, and the base pressure was below 10^{-10} Torr. Metal depositions, measured by a quartz crystal microbalance, were evaporated from a tungsten coil after cleaving the GaP in vacuum. Each metal source was thoroughly outgassed prior to cleavage. The chamber pressure during evaporation or when open to the beamline was maintained below 3×10^{-10} Torr, and the valence-band spectra were monitored to assume that no contamination was taking place. All coverages are given in effective monolayers (ML), where 1 ML on GaP(110) is defined to be 9.52×10^{14} atoms per cm^2 , the surface density of substrate atoms. The [110]-oriented rods of single-crystal GaP were *n*-type doped with $4 \times 10^{17} \text{ cm}^{-3}$ of sulfur.

As mentioned in the Introduction, the surface potential change (band bending) is established as a function of coverage by determining shifts in the bulk component of the substrate core-level spectra. The Ga 3*d* and P 2*p* core levels were taken at photon energies of 80 and 170 eV, respectively, for maximum sensitivity to the reacted phases at the surface. In addition the P 2*p* was periodically monitored at the more bulk sensitive photon energy of 140 eV. A computer curve fitting routine¹³ was employed to subtract the background and any surface shifted¹⁴ or chemically shifted components from the spectra. The band bending determined from the surface sensitive and bulk sensitive P 2*p* spectra are in excellent agreement.

III. RESULTS

A. Interfacial chemistry

1. The noble metals: Cu, Au, and Ag

In Fig. 1 the Ga 3*d* and P 2*p* core-level spectra are presented for the interfaces of Cu, Au, and Ag on *n*-type GaP(110). For the Cu/GaP interface, signs of substrate disassociation are particularly clear in the Ga 3*d* spectra. From the lowest Cu coverage of 0.1 ML, a new component to lower binding energy signals the presence of elemental Ga. This occurs in tandem with the formation of copper phosphides, although the P 2*p* spectrum exhibits only a broadening rather than the resolution of two chemical states of phosphorus. Experiments involving Cu on InP have previously demonstrated that the formation of copper phosphides does not give a dramatic P 2*p* line-shape change from the semiconductor.¹⁵ In those experiments the photon-induced P $L_{2,3}VV$ Auger line

splitting was examined in detail to verify the formation of Cu—P bonds. In the Cu/GaP case the P 2*p* spectrum must be dominated by the reacted copper phosphide component at coverages above 10 ML because the Ga 3*d* spectra, taken at the same surface sensitivity, no longer show any sign of a component corresponding to Ga in GaP. Even the elemental Ga reaction product is buried at these higher coverages. In contrast to this interpretation, Brillson *et al.*⁹ have considered the P 2*p* spectrum to derive from the GaP substrate for all coverages. Such differences in interpretation of the interfacial chemistry inevitably lead to differences in measured band bending as discussed in further detail below.

The reaction seen in the spectra for the Au interface is analogous to that observed at the Au/GaAs(110) (Ref. 16) and Au/InP(110) (Ref. 15) interfaces. In all three cases the Au alloys with the cation, and this strongly affects the cation core-level spectra, while the anion core-level spectra exhibits a less dramatic change. At the higher coverages of Au on GaP, the Ga 3*d* core level is significantly broader than for the clean surface due to the presence of both an alloyed Ga signal and the signal from the substrate. For Au on both InP (Ref. 15) and GaP the P 2*p* core level exhibits a higher binding-energy component at coverages exceeding 0.6 ML. This component manifests itself in Fig. 1(b) primarily as an apparent decrease in the P 2*p* branching ratio from two to near one. At the Au/InP interface the photon-induced P $L_{2,3}VV$ Auger spectra have revealed that no Au—P bonds are formed at this interface,¹⁵ consistent with the strongly positive heat of reaction for Au₂P₃ formation as reported by Williams *et al.*¹⁷ The higher binding-energy P 2*p* component then presumably originates from segregated elemental phosphorus formed at the Au/InP and Au/GaP interfaces. The surface reaction may be driven by the energy of Au-cation alloying as discussed by McGilp for Au/InP.¹⁸ We note that Chiaradia *et al.*⁸ provide a different interpretation of the Au/GaP chemistry: they assert that the interface is unreactive at all coverages except for some weak interdiffusion.

For the Ag/GaP interface not much line-shape change is observed in the P 2*p* spectra as the coverage is incremented, but the Ga 3*d* spectra above 1 ML coverage are best fit with a weak shoulder on the low binding-energy side. It is clear from the spectra in Fig. 1 that the Ag is not as strongly reactive with GaP as Cu or Au. Ag has been found to be unreactive with GaAs(110) as evidenced by the absence of any new Ga 3*d* or As 3*d* components in the photoemission spectra taken at this interface,¹⁹ but the interface between Ag and InP exhibits a distinct reaction.²⁰ For both Ag/InP and Ag/GaP, the P 2*p* line shape does not exhibit much change, but a low binding energy component is seen in the cation core levels for coverages exceeding 1 ML. Silver phosphide (AgP₂) formation at these interfaces is unlikely, again due to the positive heat of the bulk reaction.¹⁷ By analogy to the Au/InP interface, Babalola *et al.*²⁰ conclude that at the Ag/InP interface some In alloys with the Ag while elemental P is released into the Ag. However, it is surprising that the P 2*p* does not then exhibit a high binding-energy elemental component similar to that seen at the

Au interface, either for InP or GaP. Apparently a stronger reaction such as at the Au interfaces is required to liberate a detectable quantity of elemental phosphorus. For the Ag/GaP interface we will tentatively conclude that some Ga alloys with the Ag, and the heat of alloying may drive this reaction. The core-level attenuation with coverage shows that Ag clusters more strongly on GaP than Cu or Au, as expected for a less reactive overlayer.

2. The transition metals: Pd and Ni

The evolution of the Ga 3d and P 2p spectra upon deposition on Pd and Ni are presented for selected cover-

ages in Fig. 2. In both cases the P 2p spectra show the presence of a higher binding-energy component at coverages exceeding 1 ML, although the Ni depositions were unfortunately not carried out to a coverage at which the reacted P 2p component is comparable in intensity to that of the bulk component. This reacted component signals the formation of palladium and nickel phosphides and is accompanied by the liberation of elemental Ga, which may be phase segregated or alloyed with the overlayer. The appearance of a low binding-energy component in the Ga 3d spectra for coverages above 1 ML supports this view.

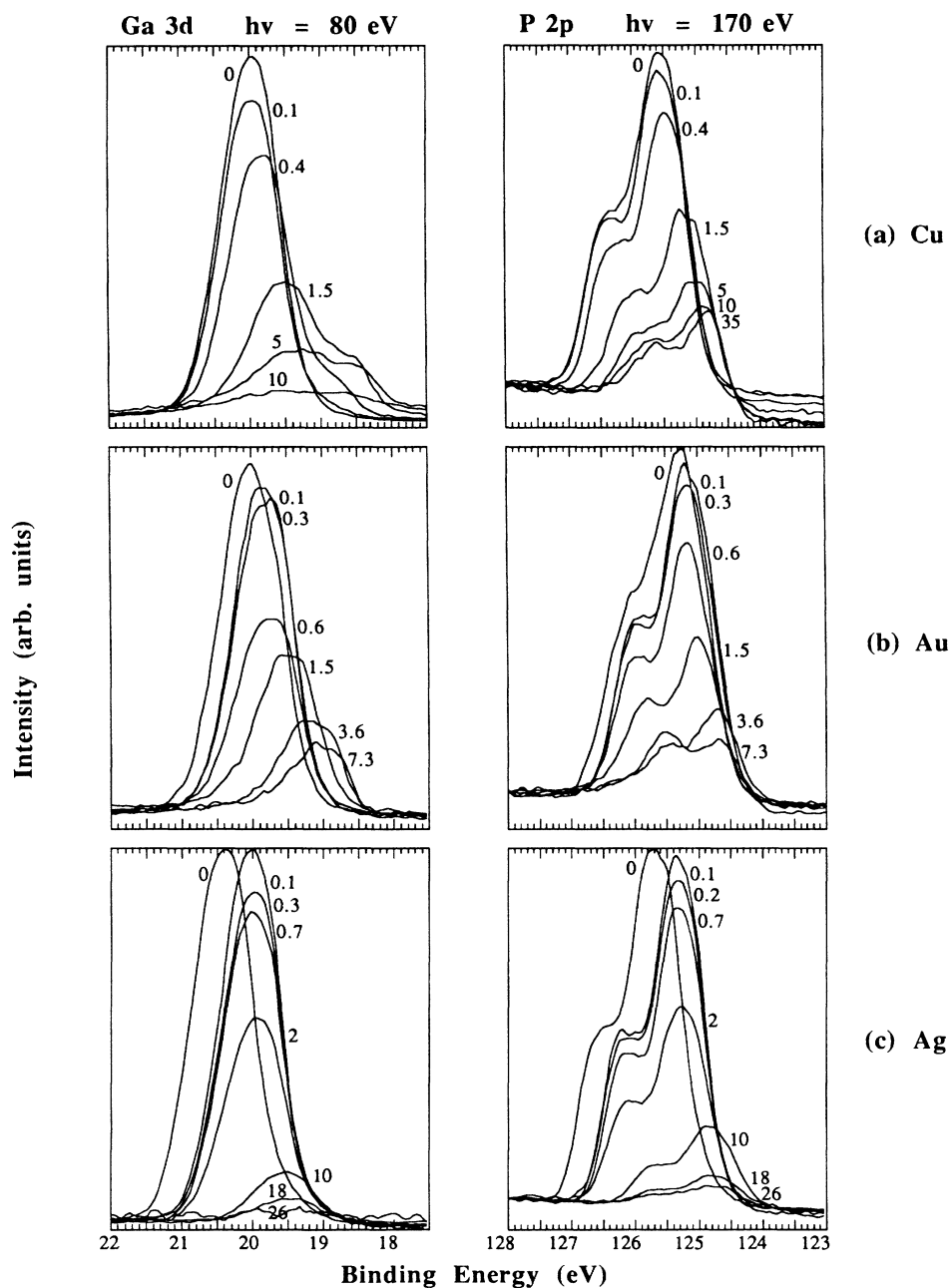


FIG. 1. The Ga 3d and P 2p core-level spectra are presented for incremental coverages of (a) Cu, (b) Au, and (c) Ag on *n*-type GaP(110). All coverages are given in effective monolayers (ML).

This palladium and nickel phosphide creation, accompanied by the ejection of the cation, is similar to that reported for InP,^{21,22} while analogous arsenide formation has been reported for the Pd/GaAs (Ref. 23) and Ni/GaAs interfaces.²² The bulk core-level intensity is attenuated rapidly as a function of Pd or Ni coverage, indicating that the overlayer does not cluster significantly. This uniformity of the overlayer is typical of reactive systems and in contrast to the unreactive Ag/GaP system, which exhibits strong clustering.

3. The column III metals: Al, Ga, and In

Figure 3 shows the Ga 3*d* and P 2*p* core-level spectra at several coverages of these column III metals. In the case of Al, the Ga 3*d* spectra exhibit the development of a lower binding-energy component, which again is indicative of segregated elemental Ga. This cation liberation has previously been reported at the Al/GaAs (Ref. 24) and Al/InP (Ref. 25) interfaces and is the consequence of a cation replacement reaction. In the case of Al/GaP,

the change in the Gibbs free energy ΔG is -10.6 kcal in going from 1 mol of Al and 1 mol of GaP to 1 mol each of Ga and AlP,²⁶ and so the reaction is not surprising. Note that the chemical shift in the P 2*p* core level between GaP and AlP is not resolved. A simple tight-binding calculation for these two semiconductors confirms that the charge transfer is very similar across the Ga—P and Al—P bonds.²⁷ In contrast to the reactive Pd/GaP and Ni/GaP interfaces, this interface seems to exhibit islanding as well, as is evidenced by the fairly strong bulk core level intensities of Ga 3*d* and P 2*p* at 19.0 and 12.6 ML coverages, respectively.

As expected, Ga on *n*-type GaP is a nonreactive interface. The Ga 3*d* spectra are a convolution of the substrate-derived components and signal from the overlayer material, while the P 2*p* spectrum exhibits a rigid shift with no new chemical states appearing. In addition the overlayer Ga exhibits extensive clustering, and consequently the Ga 3*d* and P 2*p* spectra can be analyzed into surface and bulk components even for the highest coverage of 37.3 ML.

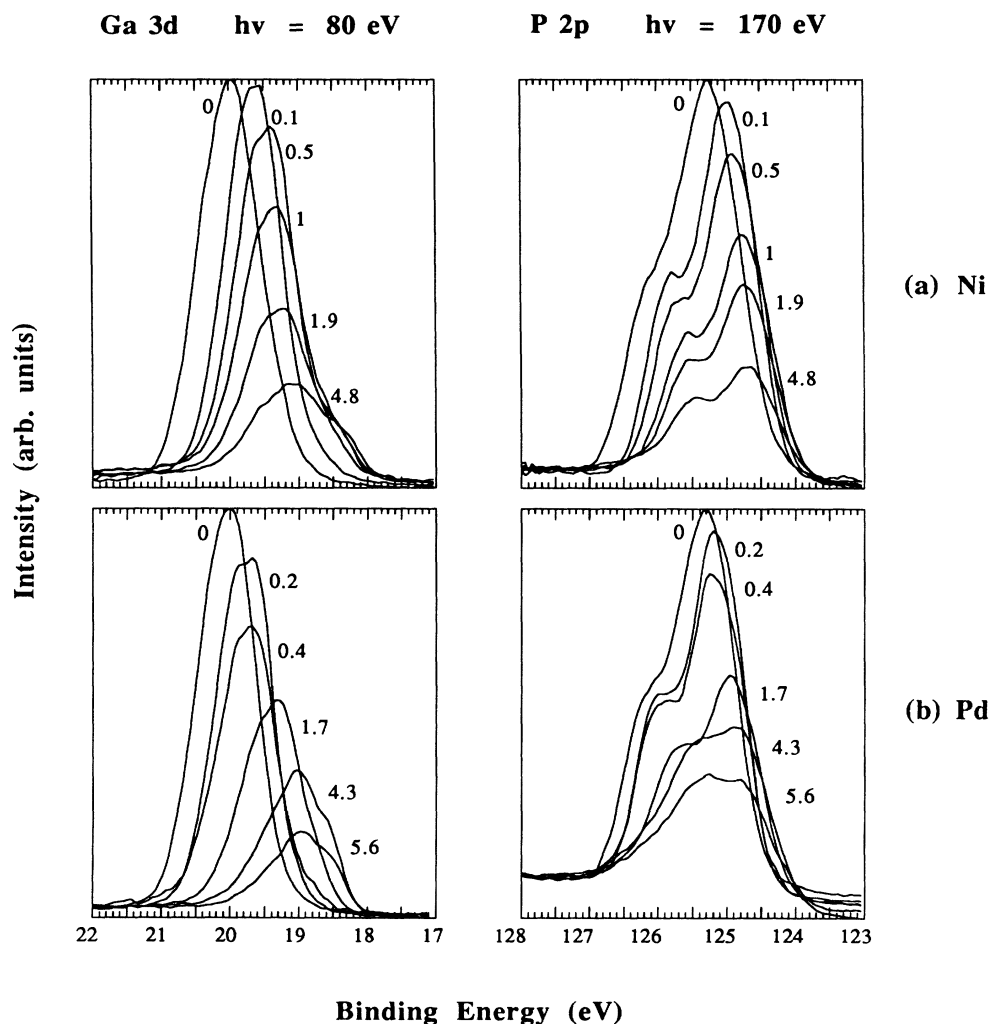


FIG. 2. The Ga 3*d* and P 2*p* core-level spectra are presented for incremental coverages of (a) Ni and (b) Pd on *n*-type GaP(110).

From bulk thermodynamics no replacement reaction is expected to occur at the In/GaP interface: ΔG is +6.16 kcal/mol in going from In/GaP to Ga/InP.²⁶ In fact no elemental Ga component arises in the Ga 3*d* spectra: the spectra are analyzed into Ga 3*d* surface and bulk components, a metallic In 4*d* component, and a chemisorbed In 4*d* component. We acknowledge that a weak elemental Ga component could be masked by the overlayer In 4*d* contribution, but studies at the In 4*d* Cooper minimum ($h\nu \approx 140$ eV) have shown that no such com-

ponent exists at the analogous In/GaAs interface.²⁸ The P 2*p* core level exhibits no new chemical components, although the case of Al/GaP demonstrated that this absence does not rule out a replacement reaction. The slow substrate signal attenuation is indicative of strong In clustering at this interface.

4. Sn, a column IV overlayer

The Ga 3*d*, P 2*p*, and Sn 4*d* core-level spectra were taken as the Sn/GaP interface was formed, and these are

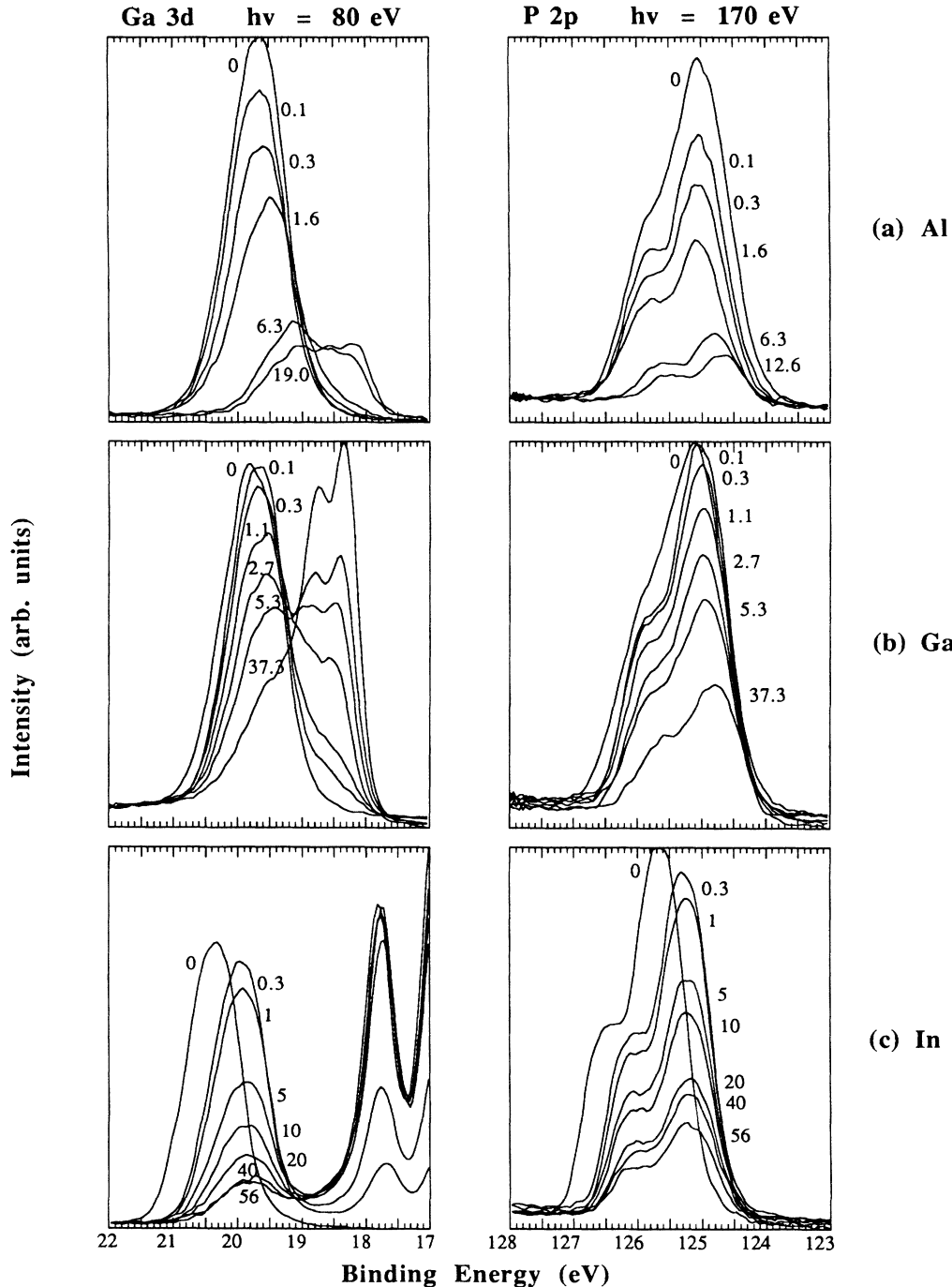


FIG. 3. The Ga 3*d* and P 2*p* core-level spectra are presented for incremental coverages of (a) Al, (b) Ga, and (c) In on *n*-type GaP(110).

presented in Fig. 4(a). The initially rapid and subsequent much slower attenuation of the substrate signal indicates that the overlayer grows in a Stranski-Krastanov fashion; that is, the first monolayer or two grows in a laminar fashion, followed by the nucleation of three-dimensional Sn islands. The appearance of a high kinetic energy shoulder in the Ga 3d spectrum indicates that the Sn disassociates the substrate somewhat, and such reactions have recently been observed for the Sn/InP system as well.²⁹ In both cases broadening of the cation core level is observed, indicating the liberation of some elemental In or Ga atoms, but the P 2p core level shows no sign of a reacted or elemental component. Such a component might be expected to appear at the same time as the elemental cation, but we have observed already in the cases of Ag/GaP and Ag/InP that the elemental cation signal can be significantly stronger. Perhaps the elemental phosphorus forms small clusters or desorbs from the surface, although these speculations must be investigated further. The P 2p surface component is attenuated with Sn deposition, and near 1 ML coverage only the bulk component of the spectrum remains. This P 2p narrowing indicates that the Sn primarily forms an ordered overlayer on the GaP or InP, thereby unrelaxing the top-layer substrate atoms and removing the surface component. The Ga 3d signal derived from the GaP loses its surface component as well, but this narrowing is masked by the appearance of the elemental Ga signal.

The Sn 4d core level is broadest at submonolayer coverages because the Sn atoms are equally divided between two chemical states: the adatoms are bonded either to the substrate Ga or the substrate P atoms. As discussed above, three-dimensional Sn islands form upon the ordered first monolayer, and in this growth regime the Sn 4d narrows and shifts to lower binding energy. Most of the band bending as determined from shifts of the Ga 3d and P 2p core levels occurs in this coverage range as well. Two opposing interpretations of the Sn 4d, Ga 3d, and P 2p shifts are as follows: (i) the Sn overlayer develops metallic character during the islanding, as reflected by the Sn 4d shift, and as a result the GaP bands bend, or (ii) an unspecified source of interface charge gives rise to substrate band bending, as reflected by the shifts in the Ga 3d and P 2p, and this band bending shifts the Sn 4d as well. The Sn 4d core level will shift with the GaP band bending only if the Sn overlayer lacks the metallic character is screen the field from the substrate depletion. Büngens *et al.*³⁰ have studied the Stranski-Krastanov growth of Sn on GaAs(110) using ellipsometric techniques and have concluded that on GaAs the Sn islands grow in the β -metallic phase. By analogy we suspect that the Sn 4d shifts for Sn on GaP primarily reflect the development of metallic character in the overlayer. A future method to definitely distinguish band bending and metallization shifts in the Sn 4d core level is to examine Sn-*p*-type GaP interfaces as well.

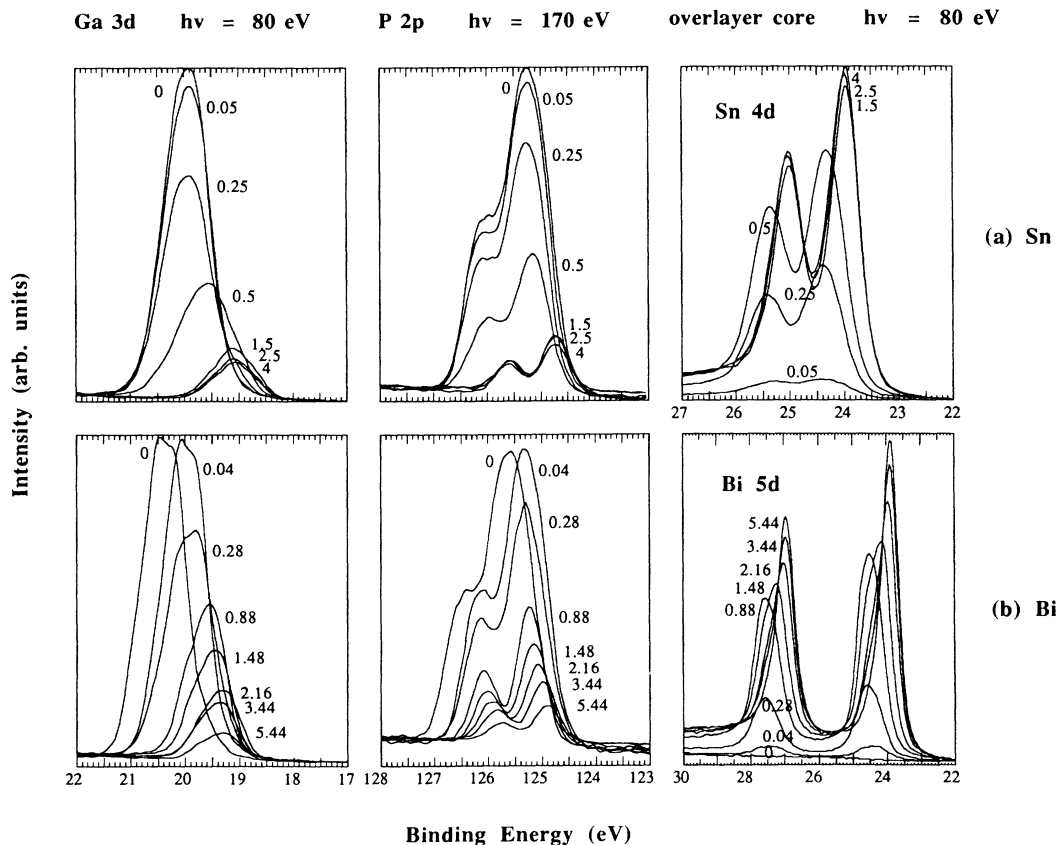


FIG. 4. The Ga 3d and P 2p core-level spectra are presented for incremental coverages of (a) Sn and (b) Bi on *n*-type GaP(110). In addition core levels from the overlayer are given for each interface.

5. Bi, a column V overlayer

When Bi was deposited on *n*-type GaP(110) the Ga 3*d* and P 2*p* core levels narrowed dramatically up to a coverage of 1 ML as exhibited in Fig. 4(b). In analogy to interfaces between Sb and III-V semiconductors such as GaAs(110) (Refs. 31 and 32) and InP(110),^{33,34} this narrowing is attributed to the removal of the surface component resulting from the formation of an epitaxial Bi monolayer and the subsequent unreconstruction of the substrate. Hence Bi provides an interesting case of a laminar unreactive overlayer. By unreactive we mean that the overlayer does not break bonds in the substrate. Above 1 ML coverage the attenuation of the Ga 3*d* and P 2*p* spectra is indicative of Stranski-Krastanov Bi growth, similar to Sn/GaP as well as the Sb-III-V interfaces.

The absence of surface components in the Ga 3*d* and P 2*p* spectra at coverages exceeding 1 ML of Bi allows the determination of various parameters for these spectra without the uncertainty of deconvolving several components.³⁵ These parameters, the Lorentzian widths, spin-orbit splitting, and branching ratio, are given in Table I, and these numbers were employed in the analysis of both bulk and surface components for all of the Ga 3*d* and P 2*p* spectra associated with this paper. The Gaussian widths depended on experimental parameters such as monochromator slit openings which varied somewhat from interface to interface.

At the higher coverages the Bi 5*d* spectra reveal a transition in the nature of the overlayer, similar to the Sn 4*d* spectra discussed above. At submonolayer coverages the Bi 5*d* is broadest due to the two chemical states of Bi atoms in the ordered overlayer. Above 1 ML a component corresponding to Bi bonded to other Bi atoms dominates the spectrum. The Bi 5*d* in this coverage regime also shifts to lower binding energy, and this shift occurs in tandem with much of the band bending seen in the Ga 3*d* and P 2*p* spectra. In contrast to Sn, the higher coverage Bi islands are certain to possess metallic character, and so the overall Bi 5*d* shift cannot be attributed to the band bending. This shift results from the formation of metallic Bi islands on the ordered Bi layer.

B. Band bending

We wish to extract from the data in Figs. 1-4 the development of the GaP barrier height and correlate this to the overlayer reactivity, morphology, and metallization, as discussed in Sec. III A. To estimate the absolute position of the surface Fermi level relative to the GaP band edges, a valence-band spectrum was taken at 80 eV photon energy on each cleaved surface prior to metal deposition. The kinetic energy of the electrons photoemitted

from the valence-band maximum (VBM) of the cleaved sample is estimated by linearly extrapolating the low binding-energy edge of the valence-band spectrum to the background as is shown in Fig. 5. This extrapolation may overestimate the value of the VBM by roughly 0.1 eV due to instrumental broadening of the actual valence-band density of states, but this error should be systematic, shifting the absolute band-bending measurements of all the interfaces by the same value.³⁶ In particular then, this method does not interfere with an investigation of trends in the barrier heights with various overlayer materials. This VBM kinetic energy is compared to the kinetic energy of electrons emitted from the Fermi level of the experimental system: this energy is taken as the inflection point in the Fermi edge spectrum taken on a thick layer of Ag in good electrical contact with the chamber and analyzer. The VBM kinetic energy is subtracted from the Fermi-edge kinetic energy to estimate the initial surface Fermi-level position relative to VBM for each cleave.

One further complication in determining the absolute barrier heights in our measurements is the suggestion of van Laar *et al.*³⁷ that acceptor surface states exist in the band gap of clean cleaved GaP, centered at 1.7 eV above VBM. These states would be occupied on cleaved *n*-type GaP and possibly merge with the valence-band spectrum. However no sign of such states is observed in the clean valence-band spectrum shown in Fig. 5. A wide range of initial pinning positions on *n*-type GaP has been observed both in this study and that of Chiaradia and Brillson *et al.*,^{8,9} including cleaves that are nearly unpinned, implying that the states in the gap of the cleaved GaP(110) surface are related to cleavage quality factors such as microsteps and are not intrinsic to this surface.

For the clean surface and following each subsequent metal deposition, the bulk component of the Ga 3*d* and P 2*p* core-level spectra is deconvolved from the surface component and the various reacted components discussed in Sec. III A. The computer curve-fitting routine¹³

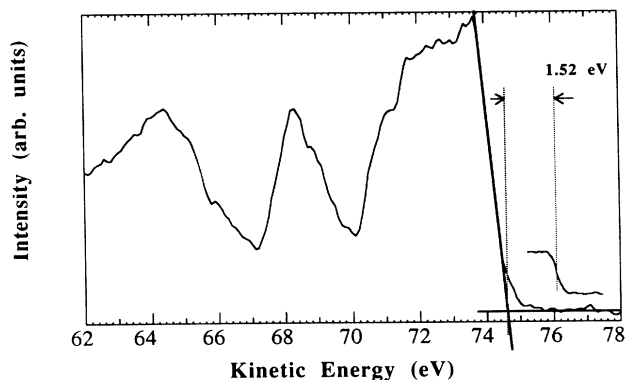


FIG. 5. Illustrated here is the procedure by which the kinetic energy of electrons photoemitted from the valence-band maximum (VBM) is determined. Superimposed is the spectrum near the Fermi edge of a thick Ag film in electrical contact with the chamber. The initial separation between the Fermi level and the VBM for this interface (Cu/GaP) was 1.52 eV.

TABLE I. Data analysis parameters as determined from 1.48 ML Bi/GaP.

Core level	Lorentzian width (eV)	Spin-orbit splitting (eV)	Branching ratio
Ga 3 <i>d</i> ($h\nu=80$ eV)	0.13	0.44	1.6
P 2 <i>p</i> ($h\nu=170$ eV)	0.06	0.87	2.0

employed the parameters given in Table I. Shifts in the bulk Ga $3d$ and P $2p$ peaks to lower binding energy are taken as a direct measurement of the increase in barrier height on this n -type material. Note that the valence-band maximum discussed above is not used as a measurement of the surface potential shift upon metal deposition because of the difficulty in deconvolving the overlayer signal from that of the substrate. For nine of the ten interfaces studied, the band bending as determined from the bulk component of the Ga $3d$ ($h\nu=80$ eV) was in good agreement with that obtained from the bulk component of the P $2p$ ($h\nu=170$ and periodically 140 eV): no systematic discrepancies exceeding 0.1 eV were observed. In the exceptional case of Au/GaP, the Ga $3d$ bulk shifts were only able to be determined up to 1.5 ML Au coverage. Beyond this coverage the spectra are impossible to decompose into a substrate-derived component and a single reacted component. Apparently the Ga that alloys with Au exists in more than one chemical state. The shifts in the Ga $3d$ and P $2p$ spectra show good agreement up to 1.5 ML, but beyond this coverage band bending is measured exclusively from the P $2p$ spectra.

This consistency within 0.1 eV of the band bending as measured from the Ga $3d$ and P $2p$ bulk components confirms our identification and deconvolution of the various chemically shifted components in the spectra. Difficulties in accounting for chemically shifted components led to larger discrepancies for the reactive overlayers of the previous GaP study,⁸ and—as discussed in

detail below—these difficulties also result in significant differences between barrier heights measured in that work and in this present one. From the consistency of the cation and anion shifts, the accuracy of our band-bending measurements is estimated to be 0.1 eV. As mentioned above the determination of the valence-band maximum position introduces a further 0.1 eV uncertainty in the surface Fermi-level position with respect to the band edges, but this uncertainty does not affect either the measured surface Fermi-level shifts (band bending) or the comparisons of thick coverage barrier heights for different overlayers.

In Fig. 6 the band bending as a function of coverage is shown for the ten interfaces of this study, with the initial and final surface Fermi-level positions summarized in Table II. As mentioned above a fairly wide range of initial band bendings—from 0.3 to 1.0 eV—was observed: such initial band bendings have been observed not to affect the high-coverage Schottky-barrier heights measured at other metal-III-V semiconductor interfaces.³⁸ Also given in Table II are the earlier photoemission measurements of Chiaradia and Brillson *et al.*^{8,9} and the electrical and photoresponse measurements of Cowley and Sze³⁹ that were performed on thick overlayer n -type GaP Schottky barriers.

The band bending for the noble metals is shown as a function of coverage in Fig. 6(a). The Au data exhibits rapid surface Fermi-level movement up to 3 ML coverage, at which point in the barrier height saturates at a

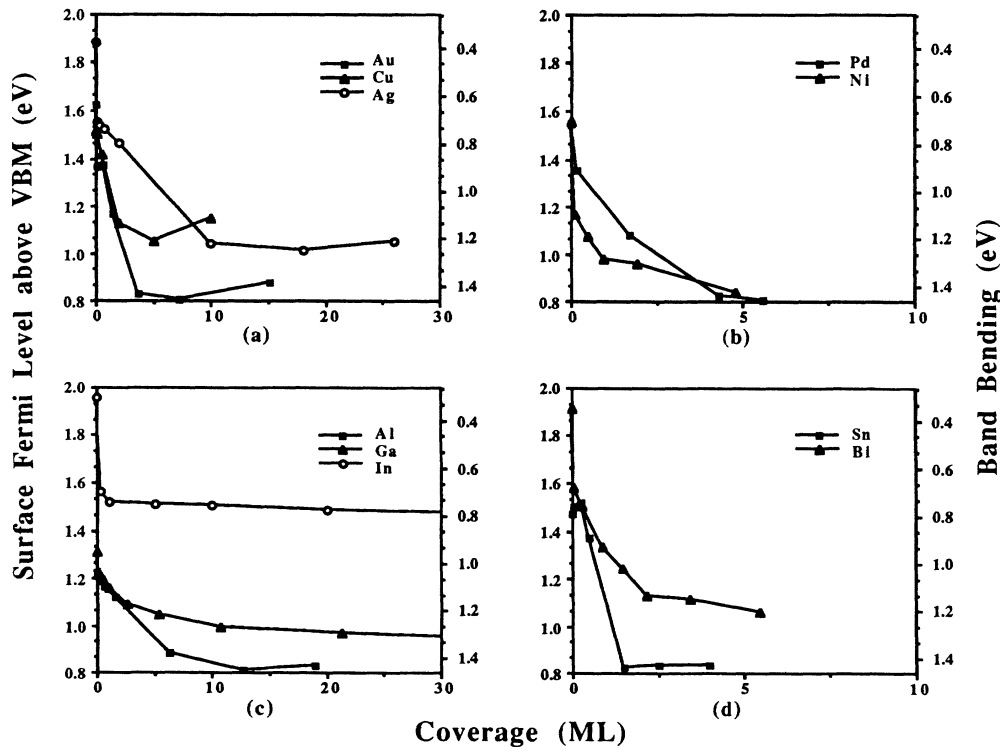


FIG. 6. Band bending as a function of coverage for various overlayers on n -type GaP(110): (a) noble metals, (b) transition metals, (c) column III metals, and (d) Stranski-Krastanov overlayers. The left axes are labeled with the surface Fermi level to VBM separation. The right axes are labeled with the conduction-band maximum (CBM) to surface Fermi-level separation, from which the final barrier height may be read.

TABLE II. Band-bending data.

Overlayer	Initial band bending from this study (eV)	Barrier height from this study (eV)	Barrier height from Chiaradia <i>et al.</i> (Ref. 8) (eV)	Barrier height from Cowley <i>et al.</i> (Ref. 39) (eV)	
				C-V	Photoresponse
Cu	0.74	1.16	1.27	1.34	1.20
Ag	0.37	1.23			1.20
Au	0.64	1.38	1.39	1.34	1.28
Ni	0.70	1.42		1.27	
Pd	0.71	1.46			
Sn	0.79	1.43			
Bi	0.35	1.14			
Al	1.04	1.44	0.73	1.14	1.05
Ga	0.95	1.32			
In	0.30	0.75	0.31		

value of 1.4 eV. Cu/GaP shows a similar rate of barrier formation, saturating at a somewhat lower barrier height of 1.2 eV. The band bending for Ag/GaP is slower than for Cu and Au, and this may be related to the reduced reactivity of Ag on GaP. More will be said in the following discussion regarding the correlations between overlayer reaction, overlayer morphology, and band-bending rate. The barrier height for Ag/GaP of 1.2 eV is achieved at a coverage near 10 ML.

In Fig. 6(b), the band bending versus coverage is shown for the reactive transition metals, Ni and Pd. The Ni and Pd interfaces both exhibited initial band bendings of 0.7 eV. The final barrier heights are also similar for the two, around 1.4 eV and are reached near 5 ML coverage. We note that these interfaces exhibit about the same band-bending rate as Cu and Au, which is again consistent with a correlation between band-bending rate and reactivity. The initial band bending proceeds somewhat more rapidly for the Ni interface although the degree of reactivity seems roughly equal at comparable coverages, judging from the core-level spectra of Fig. 2.

Figure 6(c) shows the band bending of the column III metals on GaP. The Al band bending seems slightly faster than that of the Ga, but slower than any of the other reactive interfaces. The band-bending rate of the In interface is difficult to compare because of the significantly smaller initial band bending as well as the smaller final barrier height. The Al barrier height is observed to settle around 1.4 eV, while that of the Ga is taken to be around 1.3. At coverages above 1 ML of In on *n*-type GaP, the band bending appears saturated at the unusually low value of 0.75 eV. Such a barrier height is about 0.4 eV lower than any of the others measured. Such behavior was also reported at the In-*n*-type GaAs interface⁴⁰ and may be related to unusual kinetics at these interfaces, a point will be discussed in more detail shortly. From the core-level spectra shown in Fig. 3 it is apparent that In does not react strongly with the GaP but rather clusters on the surface. We note that nevertheless the interface exhibits a very rapid initial band bending.

Figure 6(d) displays the barrier-height formation for the Sn and Bi interfaces with *n*-type GaP. As mentioned previously the major band bending for both the Sn and the Bi interfaces occurs in the coverage regime during

which metallic islands develop on top of the initial epitaxial overlayer, and the rate of this movement is comparable to the more reactive interfaces such as Ni, Pd, Cu, and Au. Neither Sn nor Bi is strongly reactive with the substrate, although the former seems to weakly dissolve the surface: hence this rapid band bending is somewhat surprising and will be discussed in further detail below. The Bi interface achieves a final barrier height of around 1.1 eV, whereas the Sn barrier height saturates at a higher value of 1.4 eV.

The coverages at which the ultimate barrier height is achieved on *n*-type GaP is generally higher than for *n*-type GaAs and *n*-type InP, again with the exception of the In interface. The barrier heights for the less reactive, clustering overlayers such as Ag, Ga, and Al stabilize at coverages above 10 ML, whereas on *n*-type GaAs the band bending stabilizes at closer to 1 ML coverage.⁴¹ The final barrier height for Ag-*n*-type InP is also established at around 1 ML.¹⁰ Similarly the reactive Pd and Ni interfaces achieve their final surface Fermi-level position at around 5 ML on *n*-type GaAs, as compared to 1 ML or below for *n*-type GaAs.^{23,41}

IV. DISCUSSION

A. Dependence of final barrier height on overlayer material

Chiaradia and Brillson, *et al.*^{8,9} claim that the barrier height, Φ_B , for metal-GaP systems is related to the overlayer work function, Φ_m , through the simple Schottky relation $\Phi_B = \Phi_m - \chi_s$, where χ_s is the semiconductor electron affinity. In particular these authors find a linear relationship with slope one between the barrier heights they measure and the overlayer work functions. This previous study includes four metals: In, Al, Cu, and Au. Two semiconductors, Si and Ge, are also included in their discussion, but the error bars for the work functions of these overlayer is of the magnitude of their band gaps since the doping of the thin films is not known. In this present study these same four metals have been investigated, in addition to six others. Recall that the Sn overlayer of this work is concluded to be metallic at the highest coverages from the narrowness and energy position of the Sn

4d core levels.

In Fig. 7(a) both our barrier-height measurements and those given in Refs. 8 and 9 are plotted versus the experimental polycrystalline metal work functions.⁴² In our data the relationship between barrier height and work function is much weaker than one-to-one with all of the barrier-heights measurements except that of In falling between 1.14 and 1.46 eV. In comparing the interfaces common to the two studies (Cu, Au, Al, and In overlayers), the barrier heights measured in this study vary less rapidly with the work function. The discrepancies here are significantly larger than the error estimated

above for these photoemission studies, and the origin of these differences is discussed next. But first we note that the additional six interfaces examined in this study give barrier heights in the neighborhood of 1.3 eV despite the one eV range of work functions in going from Ga to Ni.

It is difficult to compare the absolute numbers for barrier heights between these two studies because of uncertainties in establishing the Fermi level with respect to the band edges as discussed earlier. Chiaradia and Brillson *et al.* do not provide an explanation of their procedure in this regard, but they apparently chose their reference such that the simple Schottky relation $\Phi_B = \Phi_m - \chi_s$ was

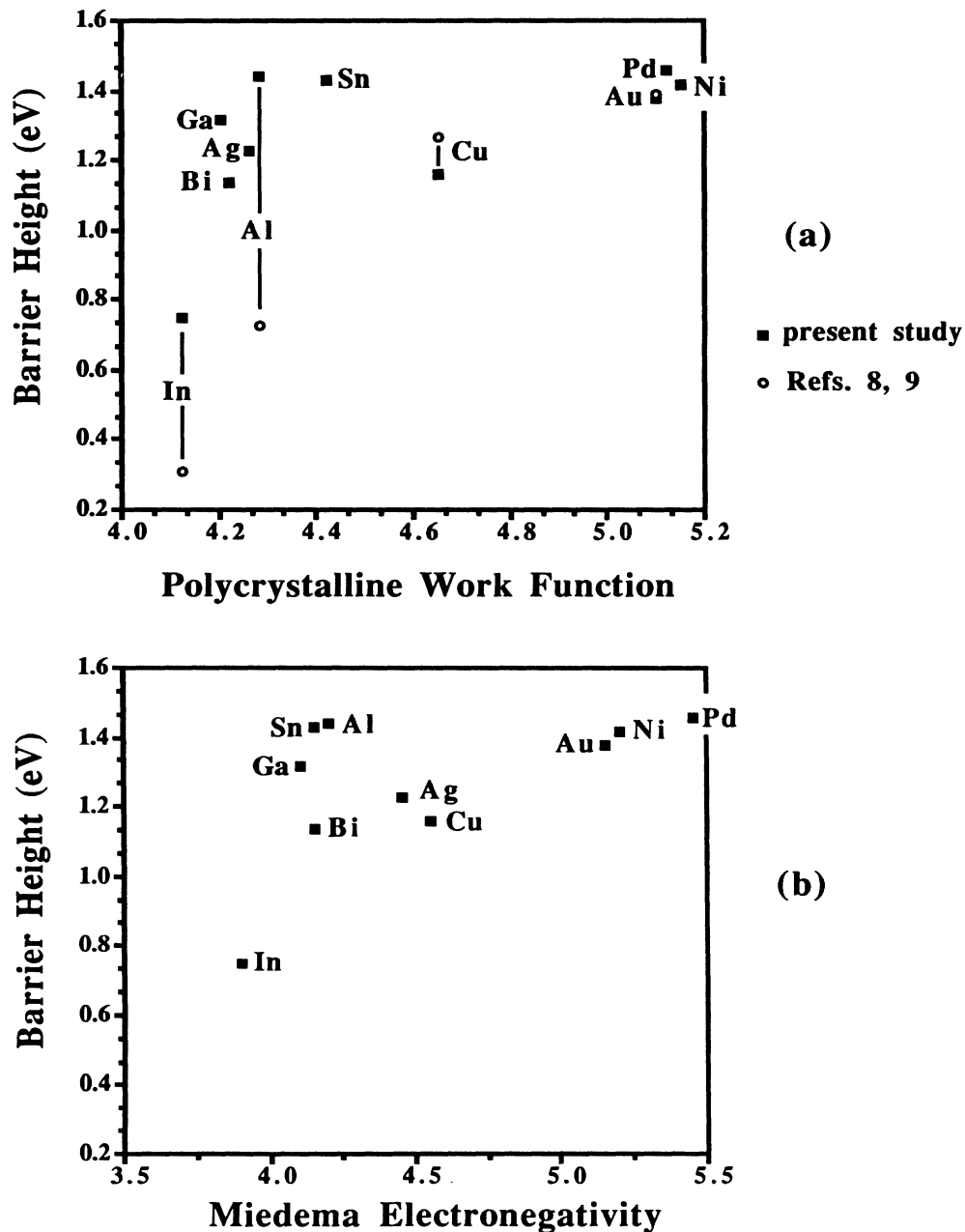


FIG. 7. The photoemission-determined barrier height for the ten interfaces on *n*-type GaP are plotted vs (a) the polycrystalline work function and (b) the Miedema electronegativity of the overlayer materials. In (a) the barrier heights determined by Chiaradia and Brillson *et al.* (Refs. 8 and 9) are also plotted for comparison.

best satisfied, using $\chi_s = 3.75$ as given in the literature.³⁷ Thus only the relative differences between the barrier heights for specific overlayers can meaningfully be compared: in other words the data points from Refs. 8 and 9 in Fig. 7(a) may have to be shifted vertically with respect to the data points of this study for a direct comparison of barrier heights for a specific overlayer.

A sizable barrier-height difference between In and Al is measured in both the previous work and in this work [0.42 eV (Refs. 8 and 9) and 0.69 eV, respectively]. The laser difference given in Refs. 8 and 9 is attributed to lesser barrier formation at their Al interface: at their maximum coverage of 10 Å (6.3 ML), the bands are still bending rapidly as seen in Fig. 3 of Ref. 8 or Fig. 6 of this paper. The Cu barrier height in the present study is found to be 0.41 eV higher than that measured for In, whereas in the previous study this difference is much larger: 0.96 eV. This discrepancy stems from the differing interpretations of the core-level chemical shifts mentioned in Sec. III A. Recall that Brillson *et al.*⁹ claim that for Cu/GaP the P 2*p* represents accurately to the highest coverages the band bending from the bulk, and in the paper of Chiaradia *et al.*,⁸ this group acknowledges a systematic discrepancy between the Ga 3*d* and P 2*p* data for the Cu interface, concluding that the P 2*p* then gives a better indication of the band bending. On the other hand we argued in Sec. III A that the P 2*p* signal at the higher coverages of Fig. 1(c) derives from copper phosphides: high-coverage shifts are observed in the P 2*p* level, but these shifts signify a stoichiometry-related chemical shift in the phosphides rather than further band bending of the semiconductor. Finally the Au barrier height with respect to In is also determined to be much higher in the previous study than the present: 1.08 eV versus 0.63 eV separation. As discussed in Sec. III A, Chiaradia *et al.*⁸ claim that the Ga 3*d* shows no sign of reaction. However we determined that use of the Ga 3*d* for band bending leads to large overestimates of barrier heights for Au on both *n*-type GaAs (Ref. 16) and *n*-type GaP because of the alloy shift and broadening of this core level. As a result only the P 2*p* bulk component was employed to determine the band bending of the higher Au coverages in this study. We conclude that the apparent strong dependence of barrier height on the overlayer work function reported in Refs. 8 and 9 for four metal-GaP interfaces is primarily due to chemical shifts in the core-level spectra. Such shifts are carefully accounted for in this study, and the barrier heights of these same four metals as well as six others is found to display little systematic dependence on the work function.

The use of the experimental work function in Fig. 7(a) may be somewhat naive because this work function includes the effects of surface dipoles on the metals, and these dipoles ought to be significantly different at the semiconductor interface. In Fig. 7(b) the barrier heights are therefore replotted against the Miedema electronegativity,⁴³ which is an attempt to account for the internal work function of the material, subtracting out the effects of surface dipoles. Again if the In data point is discounted the two factors seem unrelated, and in particular the barrier heights seem concentrated around 1.3 eV regard-

less of the overlayer. McLean *et al.*⁴⁴ recently investigated the relationship between electrically measured barrier heights on *n*-type GaAs and Miedema electronegativity and found that the data points could be divided into two groups: the overlayers with *d* valence states exhibit a barrier height constant to within 0.1 eV whereas those overlayers without such states exhibit a distinct linear dependence on the electronegativity. Of our ten overlayers all but Bi were included in the study of McLean *et al.* and all of these except Ni were categorized as belonging to the group with a linear dependence on electronegativity. Clearly no such simple division of the overlayers can be made on the basis of the data shown in Fig. 7(b).

The barrier heights measured in this study are concentrated in the same regime as the earlier thick coverage measurements performed by Cowley and Sze using capacitance voltage and photoresponse measurements.³⁹ Table II indicates that the barrier heights for metals in common to this study and Ref. 39 are in good agreement, with the exception of Al for which our barrier height is 0.3 eV higher. Further electrical measurements on ultra-high-vacuum-formed interfaces between GaP and all of these overlayers would provide a good test of the values obtained in the photoemission, and such investigations are currently being conducted.

We conclude then that the barrier heights to *n*-type GaP(110) have no systematic dependence on the overlayer work function or electronegativity but rather are restricted to a narrow range of energies. This is the type of Fermi-level pinning that has been reported previously for Schottky barriers on GaAs and InP. Brillson *et al.*⁴⁵ have suggested that in the case of GaAs, the Fermi-level pinning is due to imperfections in the bulk-grown material and that with better molecular-beam epitaxy prepared samples, a wider range of barrier heights is achieved. However, in both this study and the GaP study of Chiaradia and Brillson *et al.*,^{8,9} the substrates are melt-grown crystals, and the primary difference in the reported degree of pinning comes from the interpretation of the data rather than some inherent perfection or lack thereof in the substrate material.

B. Implications regarding GaP midgap states

As mentioned in the Introduction, two particular sources of surface states have been suggested to explain a lack of variation of barrier heights such as seen here with GaP: defects and metal-induced gap states (MIGS). The position of likely defect stabilization as established by irradiation of GaP (Ref. 46) (1.2-eV band bending on *n* type) and the theoretical charge neutrality level toward which MIGS are expected to pull the surface Fermi level⁴⁷ (1.45-eV band bending on *n*-type GaP) are both in the neighborhood of the barrier heights measured in this study, thus complicating efforts to distinguish the importance of these two effects. As with GaAs and InP we may attempt to make such a distinction through observation of the reactivity, metallization, and morphology of the overlayer and the correlation between these and the band-bending rate and final barrier height.

In order to examine the lower coverage band bending in greater detail, the curves of Fig. 6 are replotted in Fig. 8 with the coverage on a logarithmic scale. These plots are particularly interesting for the interfaces with Au, Ag, In and Bi, which exhibit an initial band bending of less than 0.7 eV. The surface Fermi level moves rapidly for submonolayer metal depositions to the neighborhood of 0.8-eV barrier height. In the cases of Au, Ag, and Bi the band bending eventually resumes at a slower pace to the final pinning position in the neighborhood of 1.3 eV. These well-cleaved interfaces then indicate that at least two distinct mechanisms may be at play in bending the *n*-type GaP bands, although only the final mechanism establishes the Schottky-barrier height. First we will briefly discuss the rapid submonolayer band bending seen at the four interfaces mentioned above.

This band bending seems to saturate near 0.8 eV despite the large electronegativity range spanned from In to Au, and thus overlayer-specific mechanisms such as adatom-induced states are ruled out as the mechanism. MIGS are often discussed even in the context of submonolayer coverages because the clustering adatoms such as Au, Ag, and In may establish metallic character even at low coverages. However, it is questionable whether such small-cluster-based MIGS would be able to saturate at 0.8 eV the band bending at the surface between the clusters,⁴⁸ and furthermore, this 0.8-eV level is far from the calculated charge neutrality level of 1.45 eV. This 0.8-eV position is also far from the irradiation-established defect position of 1.2 eV, but a second defect

level at this 0.8-eV energy is possible: thus we suggest that defects may be responsible for the rapid submonolayer band bending observed for Au, Ag, In, and Bi on *n*-type GaP. More detailed low-coverage investigations of *n*-type GaP barrier formation are of potential interest.

Next we concentrate on the mechanism for the slower band bending to the final barrier height, which with the exception of In is in the neighborhood of 1.3 eV. It was noted previously that the coverage at which this barrier height is established is higher for GaP than for GaAs and InP. This is not simply a reflection of the greater total band-bending occurring at GaP, around 1.3 eV as opposed to 0.7 and 0.4 eV for *n*-type GaAs and *n*-type InP, respectively. The interfacial charge density σ is related to the square root of the band bending, $\Delta\phi$:

$$\sigma = (2q\epsilon N_d \Delta\phi)^{1/2},$$

where N_d is the substrate doping. A ratio of two or three in barrier height translates to a factor of less than 2 in the interfacial charge required to pin the surface. Then the fact that the GaP band bending saturates at coverages ten times higher than for GaAs and InP implies that significantly fewer interfacial charge states are being created for a given overlayer coverage.

This delayed barrier establishment for GaP has one possible explanation in the context of the MIGS model. Louie *et al.*⁴⁹ and Tersoff⁶ have established that the MIGS decay length decreases with increasing semiconductor ionicity and band gap. Since GaP has a

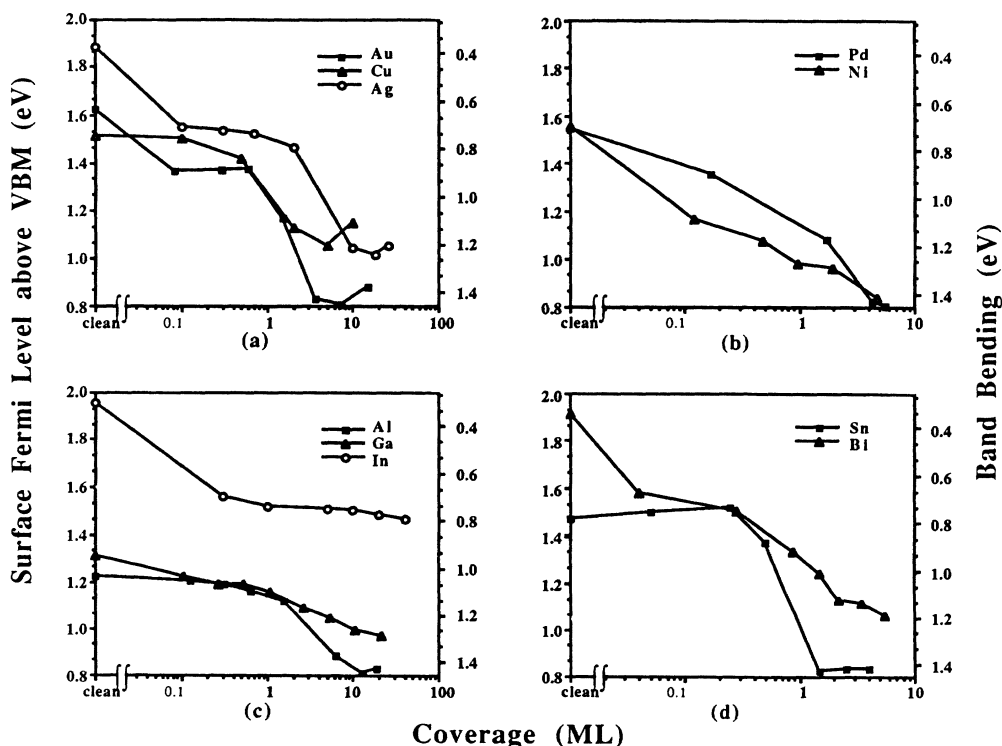


FIG. 8. The band bending as a function of coverage for the same interfaces presented in Fig. 6. In this case the coverage is given in a log scale.

significantly higher band gap than GaAs and InP [the room-temperature (RT) values are 2.26, 1.42, and 1.35, eV, respectively], a greater density of MIGS and thus a greater coverage of metal may be required to pin the Fermi level. Specific calculations of the MIGS dipole strengths are required to determine whether the greater GaP gap can account for the delay in band bending observed.

In the context of the MIGS model, another way in which the GaP band-bending rate could differ from that of other III-V's must be considered: a significantly lower GaP surface mobility would reduce adatom clustering during interfacial growth. Stiles, *et al.*¹¹ have reported a dramatic delay in the onset of MIGS at the interface between Ag and liquid-nitrogen temperature *n*-type GaAs due to such a reduction of clustering on the cold substrate. However, the photoemission spectra indicate that GaP overlayer morphology, specifically the adatom clustering, is not significantly different from that observed at RT GaAs and InP. In particular, examination of core-level attenuations, metal core level shifts and narrowing, and metal signal development at the valence band and Fermi edge have indicated that the degree of clustering of the In, Ga, Al, and Ag overlayers are not particularly different for the (110) surfaces of GaAs, InP, and GaP.

To reiterate, Stiles *et al.*¹¹ found that a reduction of clustering delays the onset of MIGS and the establishment of the Ag-*n*-type GaAs barrier height as measured by photoemission. This makes it difficult for the MIGS model to explain certain trends in the GaP barrier formation in comparing various overlayers. In particular we have pointed out before that the reactive overlayers—Au, Cu, Ni, and Pd—exhibit a faster approach to the final pinning position than do the unreactive clustering overlayers of Ag and In. This trend, slower barrier-height establishment for the more clustered interfaces, is opposite to the trend for MIGS reported by Stiles *et al.*

In fact, this particular trend may be explained more naturally in the context of a defect mechanism: the faster approach to the final pinning position exhibited by the reactive overlayers can be attributed to the rapid formation of defects because substrate atoms are being taken into the reaction and further because energy is liberated as a result of the reaction. The case of In/GaP provides an unusual case in which the band bending after the initial submonolayer stage is either extremely slow or zero despite the fact that this interface is eventually taken to coverages where nearly all of the surface is covered with metallic In (see Fig. 3). This behavior is very difficult to explain if MIGS are assumed responsible for the establishment of the other barrier heights at around 1.3 eV. It seems more probable that there is some kinetic limitation

on defect formation at this unreactive interface, as has been argued for In/GaAs.³³

Finally, the Sn and Bi interfaces, which grow in a Stranski-Krastanov fashion, must be discussed. The primary band bending at these interfaces occurs during the formation of the metallic Sn or Bi islands on top of the ordered first monolayer. The simplest interpretation of the band bending above 1 ML is that the formation of metallic islands gives rise to MIGS which determine the final Fermi-level position. Energy for defect formation may also be released during the cluster condensation, but the rate of approach of the Bi and Sn overlayers to the final pinning position is comparable to the reactive overlayers rather than that of the clustering overlayer. Further investigation of these semiordered interfaces is required to fit them into the rest of the picture.

V. CONCLUSIONS

We have examined in detail the reaction and growth mode of ten metal overlayers on *n*-type GaP(110). A detailed analysis of interfacial chemistry allowed us to properly extract the band bending and final barrier height for each of these systems. We found that for nine of the overlayers (Cu, Au, Ag, Ni, Pd, Sn, Bi, Ga, and Al), the final barrier heights are concentrated in a range from 1.14 to 1.46 eV despite the 1-eV variation in the overlayer work function. In fact we observed no simple correlation between these barrier heights and the work function. We considered the possibility of both MIGS and defects as the source of this Fermi-level pinning. Although the MIGS model can qualitatively explain the slower overall band bending of GaP as compared to GaAs and InP, the trends in band-bending rate between the reactive and unreactive interfaces are more simply explained in the context of a defect model. In particular the establishment of the In barrier height at the anomalously low value of 0.75 eV is viewed as a resulting kinetic limitation on the defect formation at this unreactive interface.

ACKNOWLEDGMENTS

The authors thank D. J. Lew for collaboration during the experiment and data analysis. Also the assistance of P. H. Mahowald and C. L. Wei in obtaining the GaP samples is gratefully acknowledged. This work is supported by the U.S. Office of Naval Research under Contract No. N00014-89-J-1083. The experiments were performed at the Stanford Synchrotron Radiation Laboratory, which is supported by the National Science Foundation through the Division of Material Science Research in cooperation with the Department of Energy.

¹W. E. Spicer, P. W. Chye, P. R. Skeath, C. Y. Su, and I. Lindau, *J. Vac. Sci. Technol.* **16**, 1422 (1979).

²W. E. Spicer, Z. Lilienthal-Weber, E. Weber, N. Newman, T. Kendelewicz, R. Cao, C. McCants, P. Mahowald, K. Miyano,

and I. Lindau, *J. Vac. Sci. Technol.* **B 6**, 1245 (1988).

³V. Heine, *Phys. Rev. A* **138**, 1689 (1965).

⁴S. G. Louie and M. L. Cohen, *Phys. Rev. B* **13**, 2461 (1976).

⁵C. Tejedor, F. Flores, and E. Louis, *J. Phys. C* **10**, 2163 (1977).

- ⁶J. Tersoff, *Phys. Rev. Lett.* **52**, 465 (1984).
- ⁷L. J. Brillson, M. L. Slade, R. E. Viturro, M. K. Kelly, N. Tache, G. Margaritondo, J. M. Woodall, P. D. Kirchner, G. D. Pettit, and S. L. Wright, *J. Vac. Sci. Technol. B* **4**, 919 (1986).
- ⁸P. Chiaradia, L. J. Brillson, M. Slade, R. E. Viturro, D. Kilday, N. Tache, M. Kelly, and G. Margaritondo, *J. Vac. Sci. Technol. B* **5**, 1075 (1987).
- ⁹L. J. Brillson, R. E. Viturro, M. L. Slade, P. Chiaradia, D. Kilday, M. K. Kelly, and G. Margaritondo, *Appl. Phys. Lett.* **50**, 1379 (1987).
- ¹⁰R. Cao, K. Miyano, I. Lindau, and W. E. Spicer, *J. Vac. Sci. Technol. A* **7**, 861 (1989).
- ¹¹K. Stiles and A. Kahn, *Phys. Rev. Lett.* **60**, 440 (1988).
- ¹²M. Prietsch, M. Domke, C. Laubschat, and G. Kaindl, *Phys. Rev. Lett.* **60**, 436 (1988).
- ¹³The curve fitting is described in T. Kendelewicz, P. H. Mahowald, K. A. Bertness, C. E. McCants, I. Lindau, and W. E. Spicer, *Phys. Rev. B* **36**, 6543 (1987).
- ¹⁴D. E. Eastman, T. C. Chiang, P. Heimann, and F. J. Himpsel, *Phys. Rev. Lett.* **45**, 656 (1980).
- ¹⁵W. G. Petro, T. Kendelewicz, I. A. Babalola, I. Lindau, and W. E. Spicer, *J. Vac. Sci. Technol. A* **2**, 835 (1984).
- ¹⁶W. G. Petro, T. Kendelewicz, I. Lindau, and W. E. Spicer, *Phys. Rev. B* **34**, 7089 (1986).
- ¹⁷R. H. Williams, V. Montgomery, and R. R. Varma, *J. Phys. C* **11**, L735 (1978).
- ¹⁸J. F. McGilp, *J. Phys. C* **17**, 2249 (1984).
- ¹⁹R. Ludeke, T.-C. Chiang, and T. Miller, *J. Vac. Sci. Technol. B* **1**, 581 (1983).
- ²⁰I. A. Babalola, W. G. Petro, T. Kendelewicz, I. Lindau, and W. E. Spicer, *Phys. Rev. B* **29**, 6614 (1984).
- ²¹T. Kendelewicz, W. G. Petro, I. Lindau, and W. E. Spicer, *J. Vac. Sci. Technol. A* **2**, 542 (1984).
- ²²T. Kendelewicz, M. D. Williams, W. G. Petro, I. Lindau, and W. E. Spicer, *Phys. Rev. B* **32**, 3758 (1985).
- ²³T. Kendelewicz, W. G. Petro, S. H. Pan, M. D. Williams, I. Lindau, and W. E. Spicer, *Appl. Phys. Lett.* **44**, 113 (1983).
- ²⁴P. Skeath, I. Lindau, C. Y. Su, and W. E. Spicer, *Phys. Rev. B* **28**, 7051 (1983).
- ²⁵T. Kendelewicz, M. D. Williams, W. G. Petro, I. Lindau, and W. E. Spicer, *Phys. Rev. B* **31**, 6503 (1985).
- ²⁶I. Barin and O. Knacke, *Thermochemical Properties of Inorganic Substances* (Springer-Verlag, Berlin, 1973).
- ²⁷Following the tight-binding theory with universal parameters outlined in W. A. Harrison, *Electronic Structure and the Properties of Solids* (Freeman, San Francisco, 1980); V_3 , the polar energy, is found to be 2.41 and 2.50 for GaP and AlP, respectively.
- ²⁸K. K. Chin, K. Miyano, R. Cao, T. Kendelewicz, J. Yeh, I. Lindau, and W. E. Spicer, *J. Vac. Sci. Technol. B* **5**, 1080 (1987).
- ²⁹T. Kendelewicz, K. Miyano, R. Cao, I. Lindau, and W. E. Spicer, *J. Vac. Sci. Technol. B* **7**, 991 (1989).
- ³⁰N. Büngens, H. Lüth, M. Mattern-Klosson, A. Spitzer, and A. Tulke, *Surf. Sci.* **160**, 46 (1985).
- ³¹P. Skeath, I. Lindau, C. Y. Su, and W. E. Spicer, *J. Vac. Sci. Technol.* **19**, 556 (1981).
- ³²F. Schaffler, R. Ludeke, A. Taleb-Ibrahimi, G. Hughes, and D. Rieger, *J. Vac. Sci. Technol. B* **5**, 1048 (1987).
- ³³C. Maani, A. McKinley, and R. H. Williams, *J. Phys. C* **18**, 4975 (1985).
- ³⁴T. Kendelewicz, R. Cao, K. Miyano, I. Lindau, and W. E. Spicer, *J. Vac. Sci. Technol. A* **7**, 765 (1989).
- ³⁵T. Kendelewicz, K. Miyano, R. Cao, J. C. Woicik, I. Lindau, and W. E. Spicer, *Surf. Sci.* (to be published).
- ³⁶R. S. List and W. E. Spicer, *J. Vac. Sci. Technol. B* **6**, 1228 (1988).
- ³⁷J. van Laar, A. Huijser, and T. L. van Rooy, *J. Vac. Sci. Technol.* **14**, 894 (1977).
- ³⁸This lack of dependence of initial band bending is discussed in detail for *n*-type GaAs(110) in K. K. Chin, R. Cao, K. Miyano, C. E. McCants, I. Lindau, and W. E. Spicer, in *Thin Films—Interfaces and Phenomena*, Vol. 54 of the *Materials Research Society Symposia Proceedings*, edited by J. Nemonich, P. S. Ho, and S. S. Lau (MRS, Pittsburgh, 1986), p. 341.
- ³⁹A. M. Cowley and S. M. Sze, *J. Appl. Phys.* **36**, 3212 (1965). The value of Ni is taken from S. M. Sze, *Physics of Semiconductor Devices* (Wiley, New York, 1981).
- ⁴⁰R. R. Daniels, T.-X. Zhao, and G. Margaritondo, *J. Vac. Sci. Technol. A* **2**, 831 (1984).
- ⁴¹A survey of GaAs(110) band-bending data will be given in R. Cao, K. Miyano, T. Kendelewicz, I. Lindau, and W. E. Spicer (unpublished).
- ⁴²H. B. Michaelson, *J. Appl. Phys.* **48**, 4729 (1977).
- ⁴³A. R. Miedema, P. F. de Chatel, F. R. de Boer, *Physica B+C* **100B**, 1 (1980).
- ⁴⁴A. B. McLean, R. H. Williams, and J. F. McGilp, *J. Vac. Sci. Technol. B* **6**, 1252 (1988).
- ⁴⁵L. J. Brillson, R. E. Viturro, C. Mailhiot, J. L. Shaw, N. Tache, J. McKinley, G. Margaritondo, J. M. Woodall, P. D. Kirchner, G. D. Pettit, and S. L. Wright, *J. Vac. Sci. Technol. B* **6**, 1263 (1988).
- ⁴⁶V. N. Brudiy and V. A. Novikov, *Fiz. Tekh. Poluprovodn.* **19**, 747 (1985) [*Sov. Phys.—Semicond.* **19**, 460 (1985)].
- ⁴⁷J. Tersoff, *J. Vac. Sci. Technol. B* **3**, 1157 (1985).
- ⁴⁸K. E. Miyano, R. Cao, T. Kendelewicz, C. J. Spindt, P. H. Mahowald, I. Lindau, and W. E. Spicer, *J. Vac. Sci. Technol. B* **6**, 1403 (1988).
- ⁴⁹S. G. Louie, J. R. Chelikowsky, and M. L. Cohen, *Phys. Rev. B* **15**, 2154 (1977).